COMPARISON OF ELECTROMAGNETIC RESPONSE IN TIME AND FREQUENCY DOMAINS

S. Kashyap and A. Louie
Electronics Division
Defence Research Establishment Ottawa
Ottawa, Ontario, Canada
K1A 0Z4

ABSTRACT

This paper is concerned with the use of time- and frequency-domain methods for computing the interaction of electromagnetic waves with simple and complex structures. An example chosen for this study is a cubic box with the top open. The Finite Difference Time Domain (FDTD) method is used for computing time-domain responses to an electromagnetic pulse (EMP), a Gaussian pulse, and a sine wave. Frequency-domain results are obtained by using a moment method solution of the electric field integral equation (EFIE). Comparison is then made, both in the frequency and time domains, on corresponding quantities using Fourier transforms. Effects of various factors – the shape of the incident waveform, discretization of the structure, and Fast Fourier Transformation – on the CPU time and the accuracy of the solution are demonstrated. Guidelines are established for obtaining an accurate response.

INTRODUCTION

Use of time-domain methods such as the FDTD for modelling a wide variety of electromagnetic interaction problems has been increasing in popularity for a number of years. Application of the FDTD method has included modelling very complex structures such as the human body, microstrip and microwave structures, radar cross-section computations and inverse scattering [1]. Response can be obtained directly in the time domain, or in the frequency domain through a fast Fourier transformation (FFT).

Frequency-domain codes such as the NEC [2] and JUNCTION [3] have also been extensively used for electromagnetic analysis of a wide variety of structures. Response obtained in the frequency domain can be converted to time domain using an inverse fast Fourier transformation (IFFT).

The choice between a frequency-domain method and a time-domain method for modelling and analyzing a specific electromagnetic interaction is not always straightforward. This paper investigates the effect of a number of factors on the accuracy of the solution obtained. These factors include incident field wave shape, structure discretization, Fast Fourier Transformation (FFT or IFFT), and computer time considerations.

PROCEDURE

A perfectly conducting cubic box with an open top is chosen for this study. A plane wave with an EMP or a Gaussian or a sinusoidal waveform is assumed to be incident on the open face of the box. The FDTD method is used to compute time-domain fields at various points inside and outside the box for incident plane waves with different waveforms. Frequency-domain response is obtained by taking a FFT of the time-domain response. The frequency-domain responses thus obtained for various waveforms are then compared with the response obtained by using the moment method implementation of the electric field integral equation (EFIE). A de-convolution with the incident waveforms results in a waveform-independent frequency response. This results in a frequency-domain comparison.

For a time-domain comparison, the results obtained with the EFIE method are transformed into the time domain using an IFFT. A convolution with the incident waveforms results in the time-domain responses. These can then be compared with the responses obtained by using the FDTD method.

Since both the FDTD method and the EFIE method have been well described in the literature only a minimal description essential for this paper is given here. The theme of this paper is the *comparison* of results obtained from the two methods, rather than the intricacies of the methods themselves.

a. FDTD Method:

The FDTD method is a direct implementation of the time-dependent Maxwell's equations:

$$\varepsilon \frac{\partial \boldsymbol{E}}{\partial t} + \sigma \boldsymbol{E} = \nabla \times \boldsymbol{H}$$

$$\mu \frac{\partial \boldsymbol{H}}{\partial t} = -\nabla \times \boldsymbol{E} \qquad \textbf{(1)}$$

The finite-difference procedure proposed by Yee [4] positioned the $\boldsymbol{E}$ and $\boldsymbol{H}$ fields at half-step intervals around a unit cell as shown in Figure 1, where $\boldsymbol{E}$ and $\boldsymbol{H}$ are evaluated at alternate half time steps, effectively giving centred difference expression for both space and time derivatives. For example, taking one of the three partial differential equations associated with each of the vector equations above gives

$$\frac{\partial E_z}{\partial t} = \frac{1}{\varepsilon}\left(\frac{\partial H_y}{\partial x} - \frac{\partial H_x}{\partial y} - \sigma E_z\right)$$

$$\frac{\partial H_z}{\partial t} = \frac{1}{\mu}\left(\frac{\partial E_x}{\partial y} - \frac{\partial E_y}{\partial x}\right) \qquad \textbf{(2)}$$

Rewriting them in finite-difference form gives:

$$E_z^{n+1}(i,j,k+\tfrac{1}{2}) = \left[\frac{1 - \frac{\delta t\,\sigma(i,j,k+\frac{1}{2})}{2\,\varepsilon(i,j,k+\frac{1}{2})}}{1 + \frac{\delta t\,\sigma(i,j,k+\frac{1}{2})}{2\,\varepsilon(i,j,k+\frac{1}{2})}}\right] E_z^n(i,j,k+\tfrac{1}{2}) +$$

$$\frac{\frac{\delta t}{\varepsilon(i,j,k+\frac{1}{2})}}{1 + \frac{\delta t\,\sigma(i,j,k+\frac{1}{2})}{2\,\varepsilon(i,j,k+\frac{1}{2})}}\left[\begin{array}{l}\frac{1}{\delta x}\left(H_y^{n+\frac{1}{2}}(i+\frac{1}{2},j,k+\frac{1}{2}) - H_y^{n+\frac{1}{2}}(i-\frac{1}{2},j,k+\frac{1}{2})\right) + \\ \frac{1}{\delta y}\left(H_x^{n+\frac{1}{2}}(i,j-\frac{1}{2},k+\frac{1}{2}) - H_x^{n+\frac{1}{2}}(i,j+\frac{1}{2},k+\frac{1}{2})\right)\end{array}\right]$$

$$H_z^{n+\frac{1}{2}}(i+\tfrac{1}{2},j+\tfrac{1}{2},k) = H_z^{n-\frac{1}{2}}(i+\tfrac{1}{2},j+\tfrac{1}{2},k) + \qquad \textbf{(3)}$$

$$\frac{\delta t}{\mu(i+\frac{1}{2},j+\frac{1}{2},k)}\left[\begin{array}{l}\frac{1}{\delta y}\left(E_x^n(i+\frac{1}{2},j+1,k) - E_x^n(i+\frac{1}{2},j,k)\right) + \\ \frac{1}{\delta x}\left(E_y^n(i,j+\frac{1}{2},k) - E_y^n(i+1,j+\frac{1}{2},k)\right)\end{array}\right]$$

where ε, μ, and σ are respectively the permittivity, permeability, and conductivity of the specified coordinates in the lattice space. δx, δy, and δz are the cell dimensions, and δt is the time between successive calculations (i.e. the time step size). For a function $F(x,y,z,t)$ of space and time, $F^n(i,j,k)$ is Yee's notation for the value $F(i\delta x, j\delta y, k\delta z, n\delta t)$.

The complete system of six finite-difference equations then provides a computational scheme: the new value of a field vector component at any point depends only on its previous value and on the previous values of the components of the other field vector at adjacent points. Thus at any given time step the computation can proceed one point at a time for a single processor or several points at a time for a machine with parallel processors.

While not the subject of this paper, the following comment on the FDTD algorithm may be of interest. The finite-difference form **(3)** is obtained from **(2)** by the approximation

$$\sigma E(x,y,z,t) \approx \sigma\left(\frac{E^{n+1}(i,j,k) + E^{n}(i,j,k)}{2}\right) \tag{4}$$

This approximation is used in many FDTD studies (e.g. [1]). Others (e.g. [5], [6]) have used the approximation

$$\sigma E(x,y,z,t) \approx \sigma E^{n}(i,j,k) \tag{5}$$

and obtained good results. The approximation **(5)**, however, may lead to instability if

$$\sigma \delta t / \varepsilon > 1 \tag{6}$$

In this work, the approximation **(4)** is used. But even if we had used approximation **(5)**, because of our special treatment of boundaries for perfectly conducting bodies we would still have had stable results. For a perfectly conducting body, we have a boundary-checking algorithm that selects the boundary faces on which to set the tangential E-fields to zero. This boundary is thus a "sharp" one of zero thickness and not a "fuzzy" one-cell-thick wall with a huge σ. For a dielectric surface, we use a "harmonic mean" method to smooth out the boundary transitional effect. Another necessary key for stability of the time-stepping algorithm **(3)** is that the time step δt is chosen to satisfy

$$c\delta t \leq \left(\frac{1}{\delta x^2} + \frac{1}{\delta y^2} + \frac{1}{\delta z^2}\right)^{-1/2} \tag{7}$$

b. EFIE Method:

Reference [7] describes a simple and efficient numerical procedure for scattering by arbitrarily shaped bodies, using the moment method to solve the electric field integral equation (EFIE). The object surface is modelled by using planar triangular patches (for example, Figure 2). Because of the EFIE formulation the procedure is applicable to both open and closed surfaces. The procedure has been applied to a wide variety of electromagnetic interaction problems and has yielded excellent correspondence between the exact formulations and other methods. In JUNCTION, the EFIE approach is extended to analyze an arbitrary configuration of conducting wires and bodies. The algorithm developed can handle wire-to-wire , surface-to-surface and wire-to-surface junctions. A modified version of JUNCTION is used here as the "EFIE method".

PLANE WAVE FORMS

In this study, the time-domain incident wave on a structure is a plane wave with one of the following three shapes:

a. the nuclear electromagnetic pulse (NEMP) [8]

$$E(t) = E_0 \frac{e^{\alpha t}}{1 + e^{(\alpha+\beta)t}} \tag{8}$$

with $E_0 = 5.126 \times 10^4$ V m^{-1}, $\alpha = 1.027 \times 10^9$ s^{-1}, and $\beta = 3.906 \times 10^6$ s^{-1} (see Figure 3a). [Note this pulse has a peak value of 50 kilovolts per metre at 10 nanoseconds, a 10 to 90 percent rise time of 5 nanoseconds, and a decay time to half-value of 200 nanoseconds.]

b. the Gaussian pulse

$$E(t) = E_0 \, e^{-\pi\left(\frac{t}{T}\right)^2} \tag{9}$$

with $E_0 = 100$ V m^{-1}, and $T = \sqrt{\pi}\,(m \cdot \delta t)$, where δt is the time step size and m is the "pulse width" parameter: when $t = m \cdot \delta t$, $E(t) = E_0/e \approx 0.37 \cdot E_0$. Figure 3b shows two different pulse widths.

c. the sine wave

$$E(t) = E_0 \sin\left(\frac{2\pi t}{N \cdot \delta t}\right) \tag{10}$$

with $E_0 = 1$ V m^{-1}, and frequency $f_0 = 1/(N \cdot \delta t)$ [$\omega_0 = 2\pi/(N \cdot \delta t)$], where N is the number of time steps of δt each, whence $N \cdot \delta t$ is the period. Figure 3c shows ten cycles of the sine pulse with a period of 5 ns, hence a frequency of 200 MHz.

Note the different abscissa and ordinate scales used in Figures 3a-3c. These three waveforms, when fast-Fourier transformed into the frequency domain, have the frequency spectra shown in Figures 4a-4c.

For the NEMP, note that the frequency spectrum reaches 1% of its peak value at about 100 MHz, 0.1% at about 220 MHz, and 0.01% at about 330 MHz. From 400 MHz

on numerical noise enters into the FFT process.

For the Gaussian pulse, note that narrower time-pulses have wider frequency spectra, and that 1% and 0.1% of peak values in frequency spectra are reached in the Gigahertz range (in our example where $\delta t \approx 4\times10^{-11}$ s). For the $m=12$ case, 1% is reached at about 1.5 GHz and 0.1% at about 1.8 GHz, and numerical noise dominates (i.e. the real signal falls below the "noise floor" value of about 10^{-15}) after 2.5 GHz. For the $m=6$ case these "break points" are about doubled.

The theoretical frequency spectrum of the sine pulse is, of course, the delta function centred at f_0. Figure 4c shows the FFT representation of $\delta(f-f_0)$, i.e. the sinc function. (Figure 4c is the only one among 4a-4c that shows a "truncation effect". In figures 3a and 3b, the time-domain values of the pulses are taken until the pulses have "gone through", i.e. until the pulse values are negligible, so the frequency spectra in Figures 4a and 4b are "complete". This is, of course, not possible in the sine wave 3c.)

FDTD RESULTS FOR AN OPEN BOX

We use, as the example in this study, a perfectly conducting cubic box with an open top, and an incident x-polarized plane wave propagating in the $-z$ direction. Each edge of the cubic box is 30 cm, and the x, y, and z coordinates range from 0 to 0.3m. The cubic box is divided into $13\times13\times13$ Yee cells, centrally located within an FDTD cell space of $60\times60\times60$ cells. Four field points are chosen for comparison between their time- and frequency-domain E_x-field responses. These points are labelled A,B,C,D and are at a distance of 0.0577m from the "$x=0$"-wall, 0.1385m from the "$y=0$"-wall, and 0.0923, 0.2077, 0.3000 (at the "mouth" of the box), and 0.5077 ("outside" the box) metres from the bottom ($z=0$) of the box, respectively. Since each cubic Yee cell has an edge length of 0.3m/13 = 0.0231m, these field points are 2.5 space steps from the "back", 6 space steps from the "side", and, respectively, 4, 9, 13, and 22 space steps from the bottom. [The x-coordinates are half a space step off because in the Yee cell, the E_x-field component is evaluated at $(x+\delta x, y, z)$.] Figure 5 shows the boundary faces of this open box, on which the tangential E-fields are set to zero.

Figures 6-8 show the time-domain E_x-field response, at the selected field points, to incident NEMP, Gaussian, and sine pulses.

Figures 9-10 show the frequency-domain E_x-field response at the selected field points, obtained from a fast Fourier transformation with de-convolution of the incident pulse of the corresponding time-domain curves in Figures 6 and 7. For the responses to the NEMP in Figure 6, since it was too time-consuming to run FDTD for enough time steps for them to decay down to close-to-zero values, they are extrapolated for later time

using a simple exponential decay curve. (It is necessary in the time-to-frequency Fourier transform for the time-domain function values to reach close to zero for the Fourier integral not to be "truncated".) The magnitude of the frequency response (in this case at 200 MHz) corresponding to the sine pulse in Figure 8 are simply the stationary time-domain response peak values (also shown in Figure 8).

The corresponding curves in Figures 9 and 10 compare reasonably in an overall qualitative way. The excessive "wiggling" of the curves in Figure 9 beyond 300 MHz is due to the numerical noise in the FFT-frequency spectrum of the NEMP curve for higher frequencies (as noted above). Thus the results in Figure 9 are only reliable up to about 300 MHz. Because for the Gaussian pulse (with $m = 12$) numerical noise does not set in until after 2.5 GHz, we may be tempted to "trust" the results in Figure 10 for the whole domain (up to 1.75 GHz) shown. There is, however, another limitation in force. The spatial resolution of the FDTD box is 0.0231m, and so for reasonable accuracy the minimum wavelength should be $10 \times 0.0231 = 0.231$m, whence the maximum frequency is 1.3 GHz.

Thus, in the domain 0-300 MHz, the corresponding curves in Figures 9 and 10 are identical. Also, the frequency responses obtained from the time-domain incident sine wave in Figure 8 match these curves at 200 MHz. We may therefore conclude that any one of the incident waves may be used to run FDTD, and *within the numerically reliable part of their frequency spectra*, the fast-Fourier transformed response in frequency domain are comparable. From a computational-time standpoint, it is therefore more efficient to run FDTD with the Gaussian pulse, as less time steps are needed for completion (i.e. for the response fields to decay to close-to-zero values).

EFIE RESULTS AND COMPARISON IN FREQUENCY DOMAIN

For the EFIE method in the frequency domain, the same open-topped box is used, subjected to an incident E_x-polarized plane wave travelling in the $-z$ direction at various frequencies. Several geometric versions of the box are used, representing various resolution requirements: recall the one-fifth wavelength rule, that the maximum edge length on the structure must be at most one-fifth of the incident wave length for the field results to have reasonable accuracy. Two versions are shown in Figure 11.

There are two different ways to represent the frequency-domain response field data. One way is for a fixed field point, EFIE is run for a whole domain of different frequencies (e.g. every 10 MHz step up to 1.6 GHz), and the resulting E-field versus frequency data set is directly comparable to the Fourier-transformed data from FDTD such as those shown in Figures 9 and 10. A second, more common, way is for a fixed frequency, EFIE is run for a set of field points (e.g. for the box at (0.0577,0.1385, z) where z ranges from -0.1 to 0.6 with $\delta z = 0.01$). To compare the E-field versus location data set with FDTD, the time-domain FDTD response at many field points are taken and then

Fourier-transformed to frequency domain, and one value at the particular frequency for each field point is collected.

As an example of the first type of comparison, consider the field points C = (0.0577,0.1385,0.3000) and D = (0.0577,0.1385,0.5077). For each field point, EFIE is run for every 10 MHz, from 10 MHz to 1.6 GHz, and the E_x-field values at C and D are evaluated. The results are the solid curves shown in Figure 12. The dashed curves are from FDTD, viz the curves in Figures 10c and 10d. The comparison is reasonably good, and we shall discuss the discrepancies (especially above 1 GHz) in a later section. The comparison differs from point to point and is better at D (and at other points) than at C. We shall use the "worst" point C among the four and the "good" point D for further illustration and analysis.

As an example of the second type of comparison, consider at a fixed frequency 200 MHz, the set of field points $\{(0.0577,0.1385, z)$: $-0.1 \le z \le 0.6$, with $\delta z = 0.01\}$. (Note that this field line passes through the points A-D.) EFIE is run at 200 MHz, and the E_x-field values at these points are evaluated. The result is the curve shown in Figure 13. FDTD, on the other hand, is run with (arbitrarily) nine field evaluation points. The resulting time-domain E_x-field data are then transformed to frequency domain, and $E_x(f)$ at $f = 200$ MHz at these nine points are the circles in Figure 13. It makes no significant difference in this case (i.e. at this frequency) which incident wave is used in FDTD, as we observed in the previous section. Again, the comparison is reasonable, and the minor differences will be discussed later.

COMPARISON IN TIME DOMAIN

Comparison between FDTD and EFIE can also be made in time domain. When the E_x-field versus frequency EFIE curves of Figure 12 are inverse-Fourier transformed to time domain and convolved with the Gaussian pulse, we obtain the solid curves in Figure 14, which are almost identical to the FDTD results of Figures 7c and 7d (shown as the dashed curves in Figure 14).

When the EFIE curves are inverse-Fourier transformed to time domain and convolved with the NEMP, however, we obtain the solid curves in Figure 15. At the field point D the solid curve compares well with the dashed curve, which is the FDTD result of Figure 6d. But at the field point C, the solid curve is significantly different from the dashed curve, which is the FDTD result of Figures 6c.

The key to the explanation of this apparent difficulty in time domain comparison, at the field point C when the incident plane wave is the NEMP, is in the width of the frequency spectrum. For the Gaussian pulse with $m = 12$, over the EFIE domain in Figure 12 from 0 to 1.6 GHz, the frequency spectrum just decreases from its peak value to 0.1%

(see Figure 4b). Thus the whole data set is significant in the inverse-Fourier transform. And since the solid curves and the dashed curves in Figure 12 are relatively similar, their transforms into time domain in Figure 14 are also similar. (The inverse-Fourier transform of the dashed curves in Figure 12 – i.e. of the curves in Figures 10c and 10d – are of course just Figures 7c and 7d.) For the NEMP, 0.1% of the peak value is already reached at about 220 MHz, hence only the low-frequency portion of the curves in Figure 12 are significant in the inverse-Fourier transforms. (The FDTD curves that should be used here are actually Figures 9c and 9d, but in the domain from 0 to 220 MHz Figures 9c and 10c, and Figures 9d and 10d – the dashed curves in Figure 12 – are identical.) Observe that for the field point D in Figure 12, from 0 to 220 MHz, the solid and dashed curves are very similar, and so their transforms into time domain in Figure 15 are also very similar. But for the field point C, in the domain from 0 to about 150 MHz in Figure 12, the two curves are very different, and so their transforms into time domain in Figure 15 are different. (The inverse-Fourier transforms of Figures 9c and 9d are Figures 6c and 6d, respectively.)

So the question becomes: why, as in Figure 12 for the field point C, does the frequency domain comparison not fare well for low frequencies (< 150 MHz)? Here is where the different geometric versions of the patch-model box become a factor – but not in the expected way due to the one-fifth wavelength rule.

All the EFIE results presented so far are done with the coarser box in Figure 11, i.e. the one where the edge of the cube is divided into four equal parts. In this model, the maximum-length edges are the diagonals, which are $\sqrt{2} \times 0.3/4 = 0.106$ m. Hence by the one-fifth wavelength rule this box is good for frequencies up to about 566 MHz. The other box in Figure 11 has the cubic edge divided into ten equal parts, and by the same rule is good up to about 1.4 GHz. The one-fifth wavelength rule, however, sets a limitation on *high* frequencies, and so does *not* explain the low frequency difficulties. In fact, the one-fifth wavelength rule may be more stringent than what is observed in practice. We could run the coarser box up to 1.6 GHz and the results obtained up to about 1 GHz are very similar to those from the finer box. The use of the coarser box is the reason why in Figure 12 the two curves do not match well above 1 GHz.

As it turns out, however, the box with the finer grid does give better *low-frequency* values. The reason is that in the calculation of near fields from the currents on the edges, there must be a fine enough spatial resolution in the geometric structure to reflect the highly varying field values, especially when close to boundary edges (i.e. those edges around the opened top). This "edge effect" seems to be more pronounced at low frequencies. The numbers on the dashed curves in Figure 16 represent the number of divisions of the cubic edge into equal parts. Note that there is no significant improvement in using a finer division than edge/10. Figure 17 shows the corresponding comparison in time domain. There is still significant difference between IFFT(EFIE) and FDTD.

FDTD DISCRETIZATION

One limiting feature of the Yee-cell FDTD formulation is that the various components of the electric and magnetic fields are assumed to be constant within each Yee cell, thus these field values are "discretized" in spatial steps. We have been evaluating the E_x-field component at $(x+\delta x/2, y, z)$ in EFIE, because these are the coordinates where the Yee-cell E_x-fields are attached. When we try field points with EFIE in close neighbourhoods around the points $(x+\delta x/2, y, z)$, however, we manage to get good comparison between IFFT(EFIE)*NEMP and FDTD. Here EFIE is run with the edge/10 finer grid model of the box.

For example, around a neighbourhood of the field point C = (0.0577,0.1385,0.3), we find that evaluating the EFIE E_x-field at C' = (0.0577,0.1385,0.2850) gives the best match between EFIE and FDTD in time domain. Moving the point C' slightly in the x direction yields minor variations in the E_x-field, moving slightly in the y direction yields no change, while moving in the z direction yields the most significant changes. The best match is when C' = C - (0.,0.,0.0150). See Figure 18. (We have only tried varying one spatial direction at a time for simplicity. It is entirely possible that the best match in fact occurs at a point where all three coordinates differ slightly from C.)

Similarly, for the other three field points, we find the best matches at A' = A + (0.,0.,0.0090), B' = B - (0.,0.,0.0140), and D' = D. Field point C requires the largest spatial shift for comparison because around the "mouth" of the box, the field values have the largest variations with respect to position.

Thus, the corresponding field evaluation points that give the best match in time-domain between EFIE and FDTD are within a spatial step δz in the z direction of each other (i.e. within the same Yee cell). This is accountable as "discretization error", as the FDTD fields are discrete approximations of the "smooth" EFIE fields. Figure 19 shows the origin of this discretization error. The "central differencing scheme" of the FDTD approach approximates the derivative of a smooth function $f(x)$ at a point a by

$$\frac{df}{dx}(a) \approx \frac{\delta f}{\delta x}(a) = \frac{f\left(a+\frac{h}{2}\right) - f\left(a-\frac{h}{2}\right)}{h} \qquad (11)$$

where h is the differencing interval. But the value of this "approximate derivative" is not necessarily the exact value of df/dx at a. The mean value theorem for derivatives in elementary calculus only guarantees the existence of a value a' somewhere between $a-h/2$ and $a+h/2$ with

$$\frac{df}{dx}(a') = \frac{\delta f}{\delta x}(a) \qquad (12)$$

This is why the exact match between EFIE and FDTD occurs not necessarily at the same field point but within a spatial step.

(An alternative hypothesis exists for the non-correspondence between the FDTD field point and the EFIE field point: in [9] it is stated that the discrepancy may be due to FDTD 's spatial approximation at the box surface. But this "fuzzy boundary" is an artifact of using an FDTD body with a one-cell-thick wall. Our version of the FDTD model for a perfectly conducting body, as we mentioned before, has a "sharp" boundary of zero thickness. The uncertainly in the distance of the field point from the surface of the body is, therefore, not an issue in our algorithm.)

Theoretically, therefore, if h is made smaller, the difference between a and a' may become smaller. That is to say, that if FDTD is run with smaller cells (finer resolution), the spatial difference between matching FDTD and EFIE field points will be smaller. But using *smaller* cells also means *more* cells, and then computer memory and running time become factors.

CPU-TIME CONSIDERATIONS AND MODELLING GUIDELINES

We have shown that in computer simulations of the interaction of electromagnetic waves with geometric structures, both time- and frequency-domain codes may be used. The two independent methods are comparable – as long as proper precautions are taken – and can be used as verification of the accuracy of each other.

From an efficiency, i.e. CPU-time economy, point of view, the FDTD method with an incident Gaussian pulse is the approach of choice. For the open box example, running EFIE takes about 3 hours of CPU-time on a VAX 6420 *for each frequency*, running FDTD with the Gaussian pulse (2000 time steps) takes about 6 hours, and running FDTD with the NEMP (10000 time steps) takes about 30 hours (and the latter still needs further extrapolation). Other geometric structures also have a similar CPU-time ratio, that the CPU-time taken for EFIE(one frequency) :: FDTD(Gaussian) :: FDTD(NEMP) is 1::2::10.

The reason that FDTD(Gaussian) is the most efficient is that the time-domain response decays back to zero rapidly, and that after a complete run, one can Fourier-transform the results (with de-convolution of the Gaussian pulse) and obtain the field response *for all frequencies* (within the wide frequency spectrum of the Gaussian pulse). In other words, in the time it takes EFIE to run two frequencies, the process

FFT/Gaussian [FDTD(Gaussian)] = EFIE(all frequencies)

gives the whole frequency spectrum of responses. Because frequency-domain response comparison, with FFT(FDTD) versus EFIE, has been shown to be reasonably accurate, this process is a reliable and time-saving method in obtaining frequency-domain data.

In time domain, if one simply wants the *early-time* response to the NEMP, one may run FDTD(NEMP) directly. If, however, one is in fact interested in the *late-time* EMP response, one can run FDTD(Gaussian), then Fourier-transform to frequency domain with de-convolution of the driving Gaussian pulse, and then inverse-Fourier-transform the frequency-domain response thus obtained and convolve with the NEMP; i.e. through the process

IFFT [FFT/Gaussian [FDTD(Gaussian)]] * NEMP = FDTD(NEMP).

This way, FDTD only has to be run for the small number of time steps that an incident Gaussian pulse requires, instead of the long duration of the NEMP pulse. Several EFIE runs at selected frequencies and a direct FDTD(NEMP) run (for a smaller number of time steps) can always be used as checks to insure accuracy of this approach.

Thus, in summary, the merits of the FDTD method with an incident Gaussian pulse, followed by a time-to-frequency Fourier transform, are:

a. large frequency content of the incident pulse,
b. pulse decays down to zero rapidly, minimizing running time, and
c. efficiency: one time run to obtain all frequencies.

(Note, however, there is nothing "magical" about the Gaussian pulse itself: any time-domain pulse of narrow pulse width would share the same merits. The Gaussian pulse is chosen because of its simple analytic form and because it is a "standard".) The main disadvantage is due to computer resources, that only the chosen field quantities at several specified points are written to the output (although all six field components at all the Yee cells are evaluated at each time step, due to the constraint of the size of the output file only those chosen ones are written out). The code must be run again for computation of other field components and at other points. (As a contrast, in EFIE the currents on all the edges are stored in an output file. So the field values at any other points *at the same frequency* can be calculated from this "currents file" and EFIE does not have to be rerun.)

Time-domain response comparison has some inherent inaccuracies, mainly due to the fact that difference equations are by definition *approximations* to differential equations. In FDTD versus IFFT(EFIE), care has to be taken in finding the correct field locations for direct comparisons. Frequency-to-time inverse Fourier transformation also has some inherent problems. For a complete time-domain response it is less efficient from CPU-time considerations as described before. In addition, even for early-time response determination one still has to calculate the frequency response at a large number of frequencies to obtain an accurate IFFT into time-domain.

Finally, it must be remembered that discretization errors can be significant. In the FDTD approach one must keep in mind that the minimum reliable wavelength is ten times the size of the Yee cell (hence setting the limit for the maximum reliable frequency). Also, using smaller cells (hence more cells), within the limit of the host computer, to model the geometric object may improve the accuracy of the comparison. The availability of the field quantities only at discrete points due to the lattice structure can create some problems. In the frequency-domain code EFIE, discretization affects both the high and the low frequencies: on the one hand there is the one-fifth wavelength rule we discussed, setting the limit for the maximum frequency, and on the other hand at low frequencies there must be enough spatial resolution to reflect highly varying fields in neighbourhoods of "boundary edges". It must be remembered that the discretization guidelines of "10 cells/λ" and "edges $\leq \lambda/5$" are "traditional" ones based on experience from many studies in computational electromagnetics. They are sometimes more stringent than necessary and useful results may be obtained even above the high-frequency threshold. This is why in some of our figures (notably Figure 9) we have presented the high-frequency results well above the threshold. The point of caution is that if the guidelines are violated, one must seek independent verification of the results obtained.

CONCLUSIONS

In this paper, the penetration of electromagnetic waves inside an open-topped cubic box has been studied. The FDTD code has been used to calculate the time-domain response for an EMP, a Gaussian pulse, and a sine wave. Comparison, in both time and frequency domains, has been made with the results obtained by using the frequency-domain method EFIE. Effects of various factors such as wave shape, structure discretization, and fast Fourier transformation on CPU-time and accuracy of the results were discussed. Guidelines for using the time-domain and the frequency-domain codes were suggested. It was found to be more efficient in most cases to use the time-domain method.

Acknowledgement: We would like to thank the *ACES Journal* editor and referees for their constructive comments.

REFERENCES

[1] A. Taflove and K. R. Umashankar, "The Finite-Difference Time-Domain Method for Numerical Modeling of Electromagnetic Wave Interactions with Arbitrary Structures", *Progress in Electromagnetic Research*, Elsevier, 1990.

[2] G. L. Burke and A. J. Poggio, "Numerical Electric Code (NEC) – Method of moments", *Naval Ocean Systems Centre, Technical Document* 116, 1977.

[3] S.-U. Hwu and D. R. Wilton, "Electromagnetic Scattering and Radiation by Arbitrary Configurations of Conducting Bodies and Wires", *University of Houston, Technical Report* 87-17, 1988.

[4] K. S. Yee, "Numerical Solution of Initial Boundary Value Problem involving Maxwell's Equations in Isotropic Media", *IEEE Transactions on Antennas and Propagation*, AP-14, 302-307, 1966.

[5] A. Taflove and M. E. Brodwin, "Numerical Solution of Steady-State Electromagnetic Scattering Problems Using the Time-Dependent Maxwell's Equations", *IEEE Transactions on Microwave Theory and Techniques*, MTT-23, 623-630, 1975.

[6] J. Van Hese and D. De Zutter, "Modeling of Discontinuities in General Coaxial Waveguide Structures by the FDTD-Method", *IEEE Transactions on Microwave Theory and Techniques*, MTT-40, 547-556, 1992.

[7] S. M. Rao, D. R. Wilton, and A. W. Glisson, "Electromagnetic Scattering by Surfaces of Arbitrary Shape", *IEEE Transactions on Antennas and Propagation*, AP-30, 409-418, 1982.

[8] "EMP Engineering Handbook",
NATO File No. 1460-3, November, 1989.

[9] C. Trueman, S. Kubina, R. Luebbers, K. Kunz, S. Mishra, and C. Larose, "Validation of FDTD RCS Computations for PEC Targets", *Proceedings of the IEEE Antennas and Propagation Society International Symposium, Chicago, IL, July 18-25, 1992.*

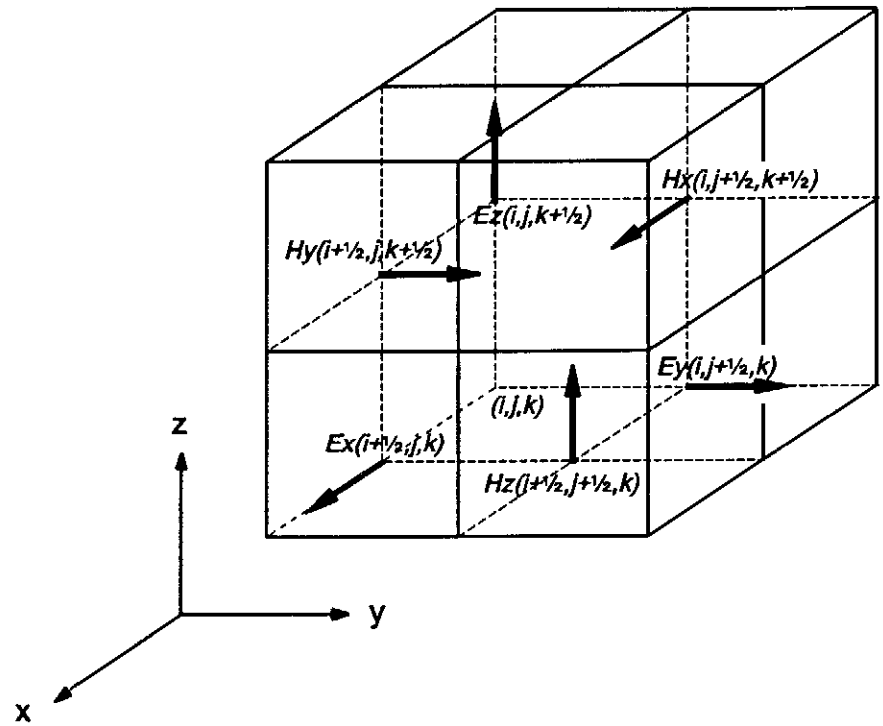

Figure 1. Position of the field components in a unit cell of the Yee lattice.

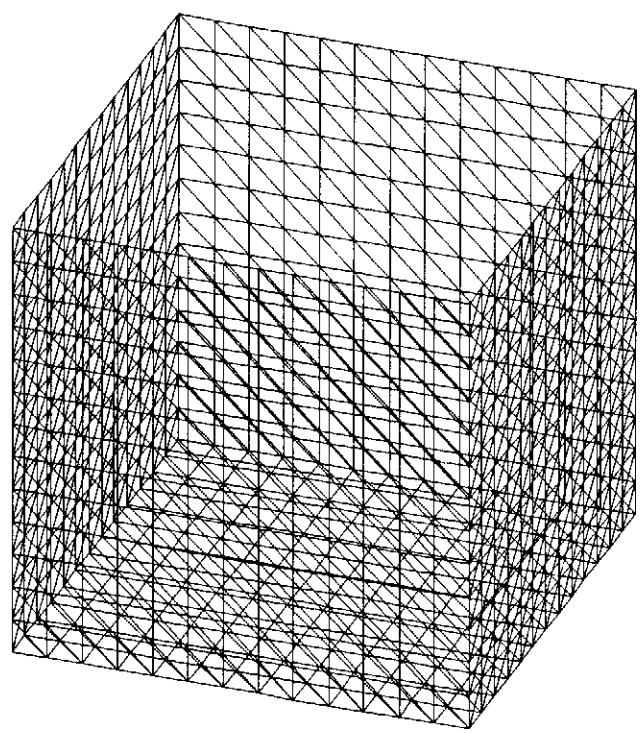

Figure 2. Example of a triangular surface-patch model input file for EFIE.

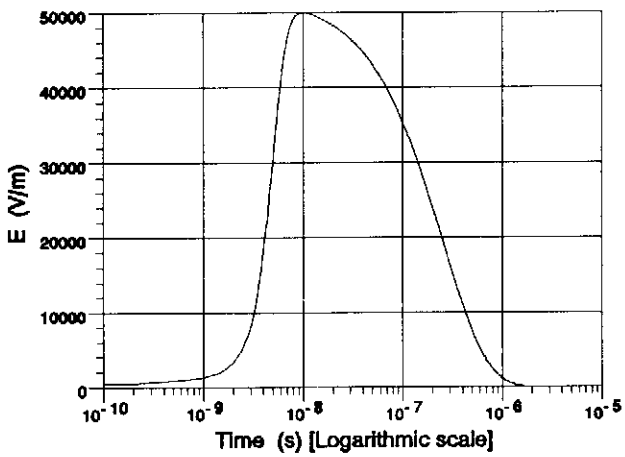

Figure 3a. NEMP in time domain

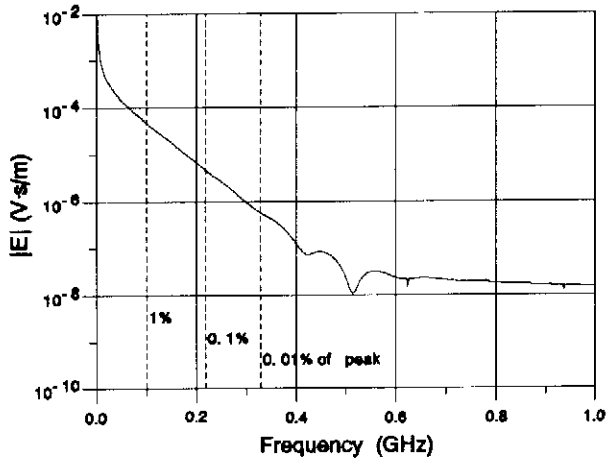

Figure 4a. NEMP in frequency domain

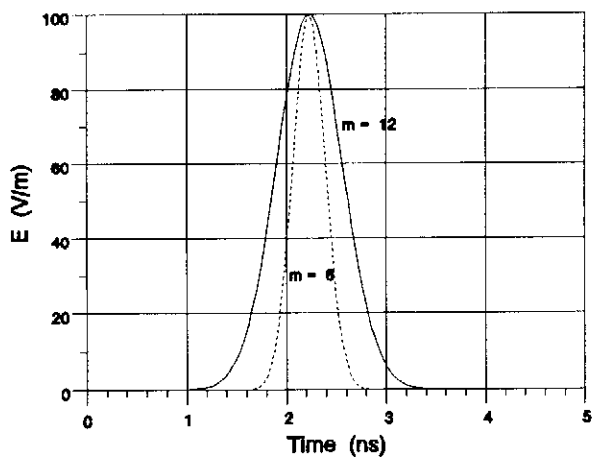

Figure 3b. Gaussian pulses with different pulse widths, in time domain

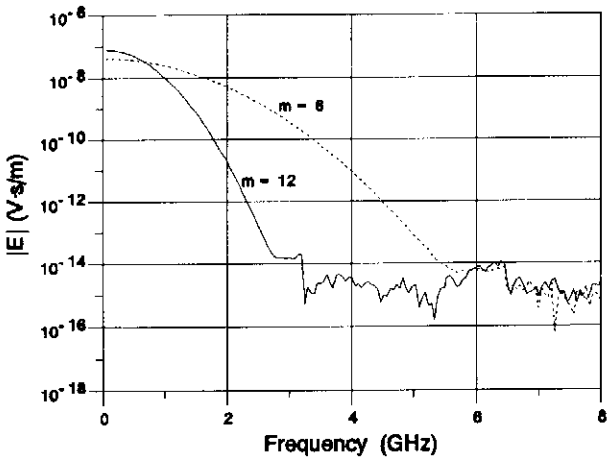

Figure 4b. Gaussian pulse with different pulse widths, in frequency domain

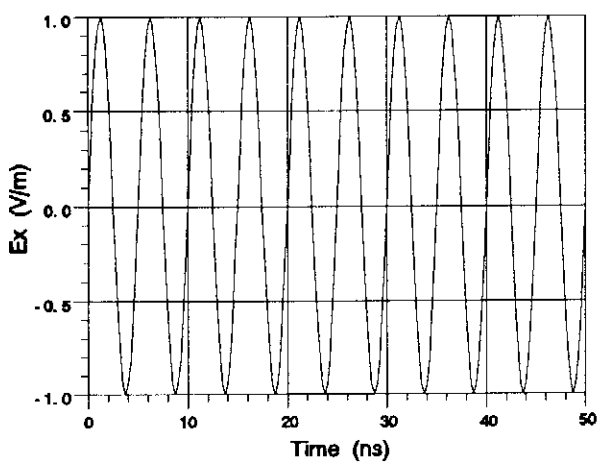

Figure 3c. Sine pulse in time domain, period = 5 ns

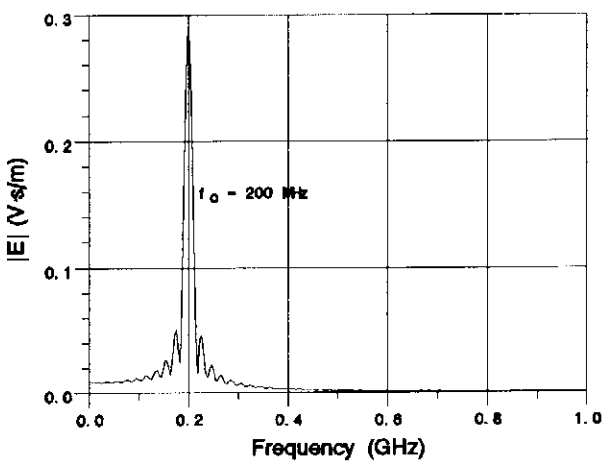

Figure 4c. Sine pulse in frequency domain, frequency = 200 MHz

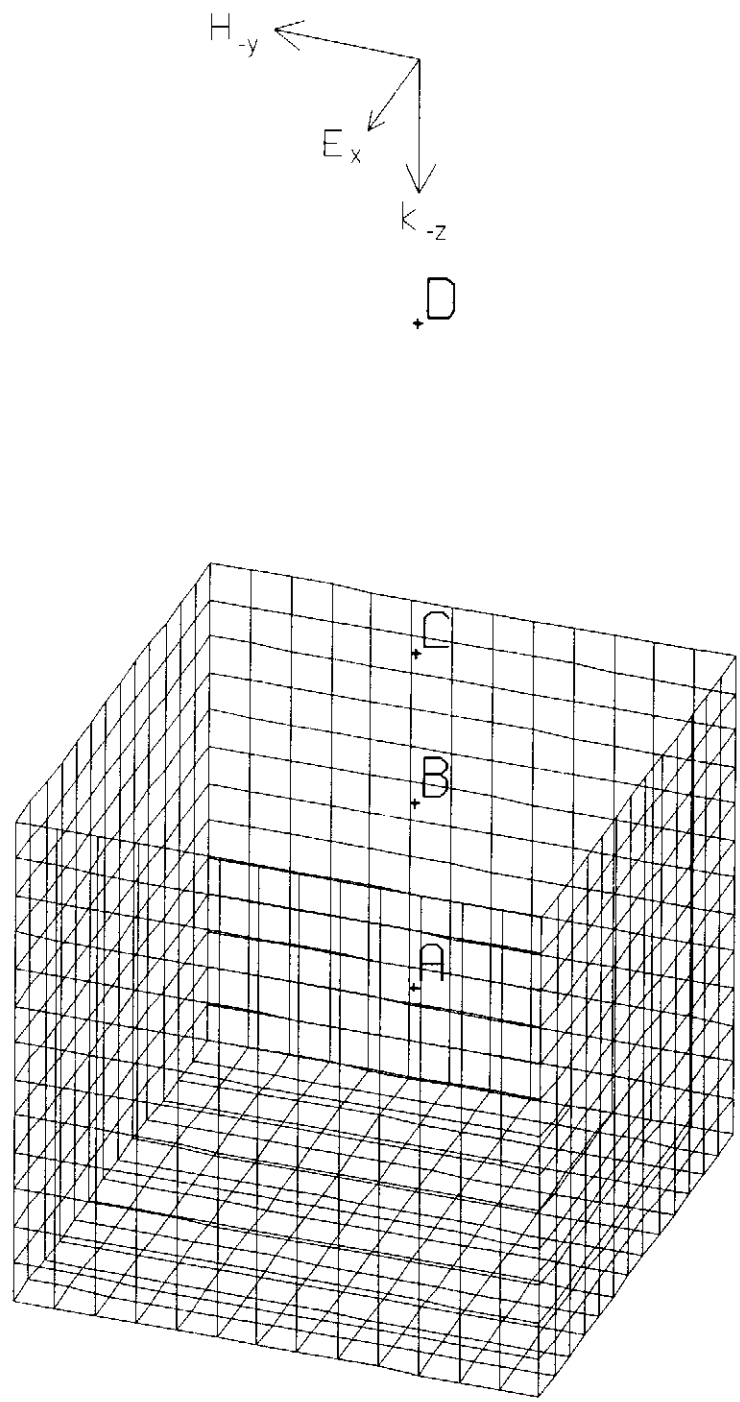

Figure 5. The open-topped box used in FDTD studies

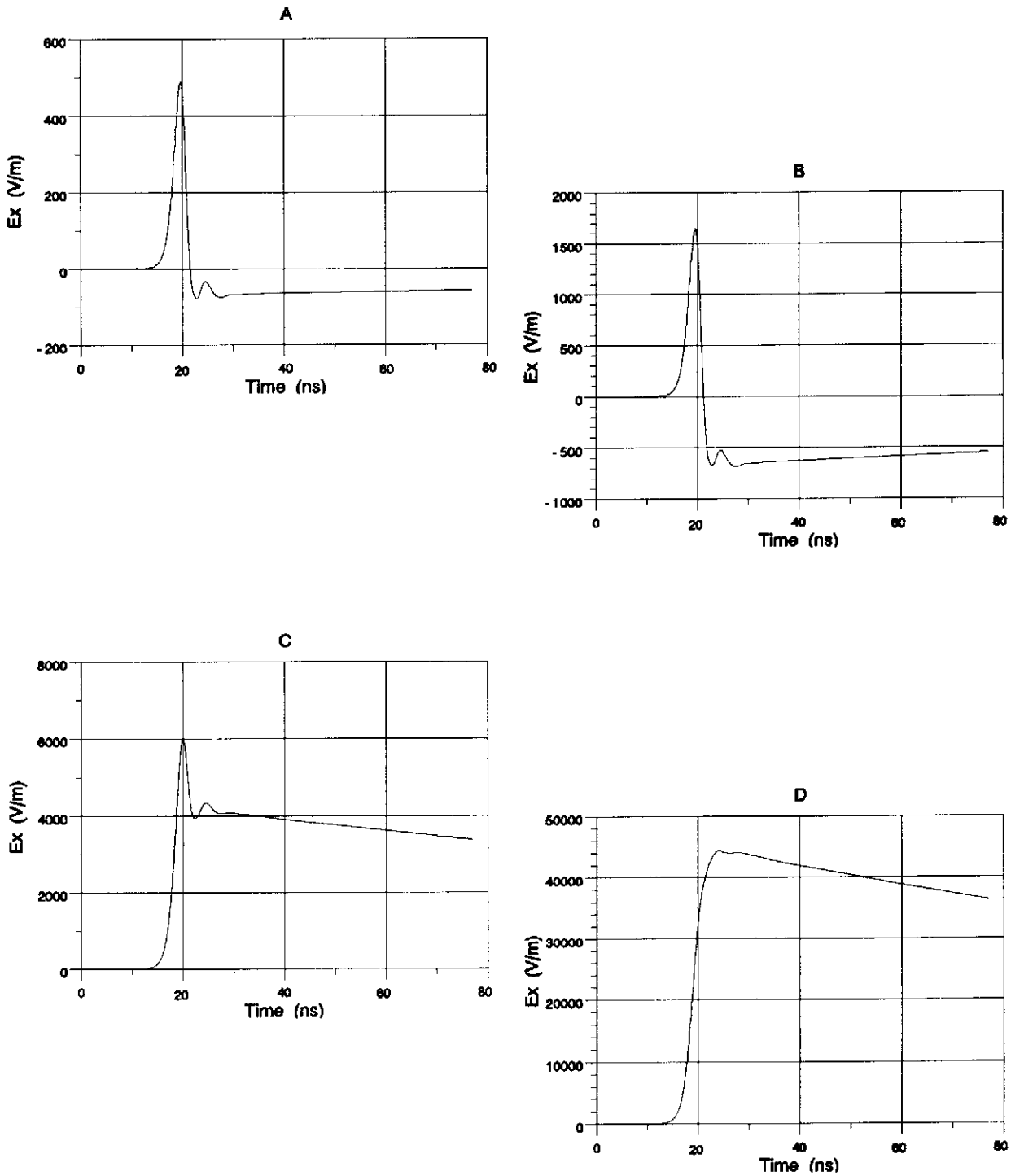

Figure 6. The Ex-field time-domain response at the four field points:
...to the NEMP,...

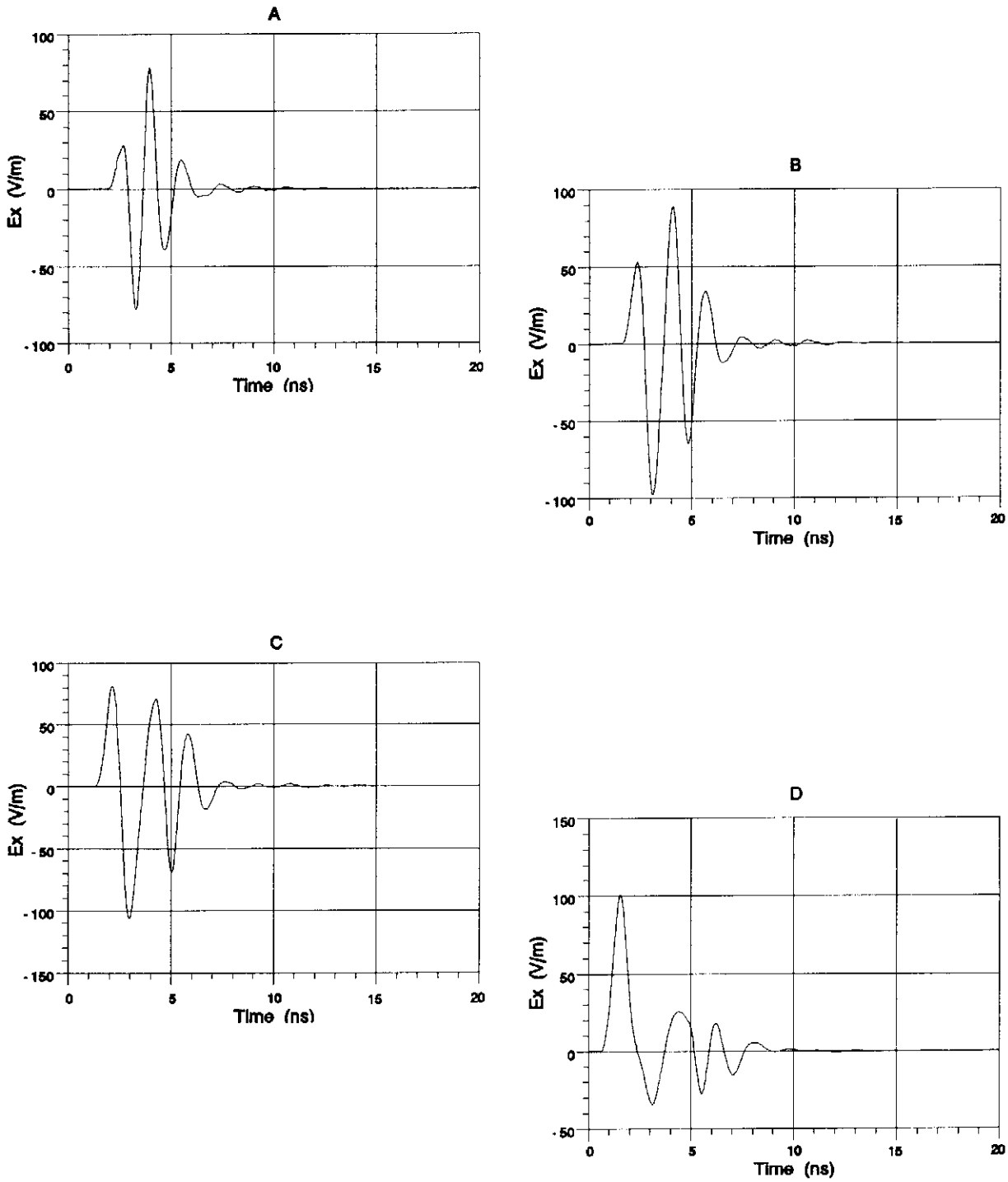

Figure 7. ...to the Gaussian pulse with $m = 12$,...

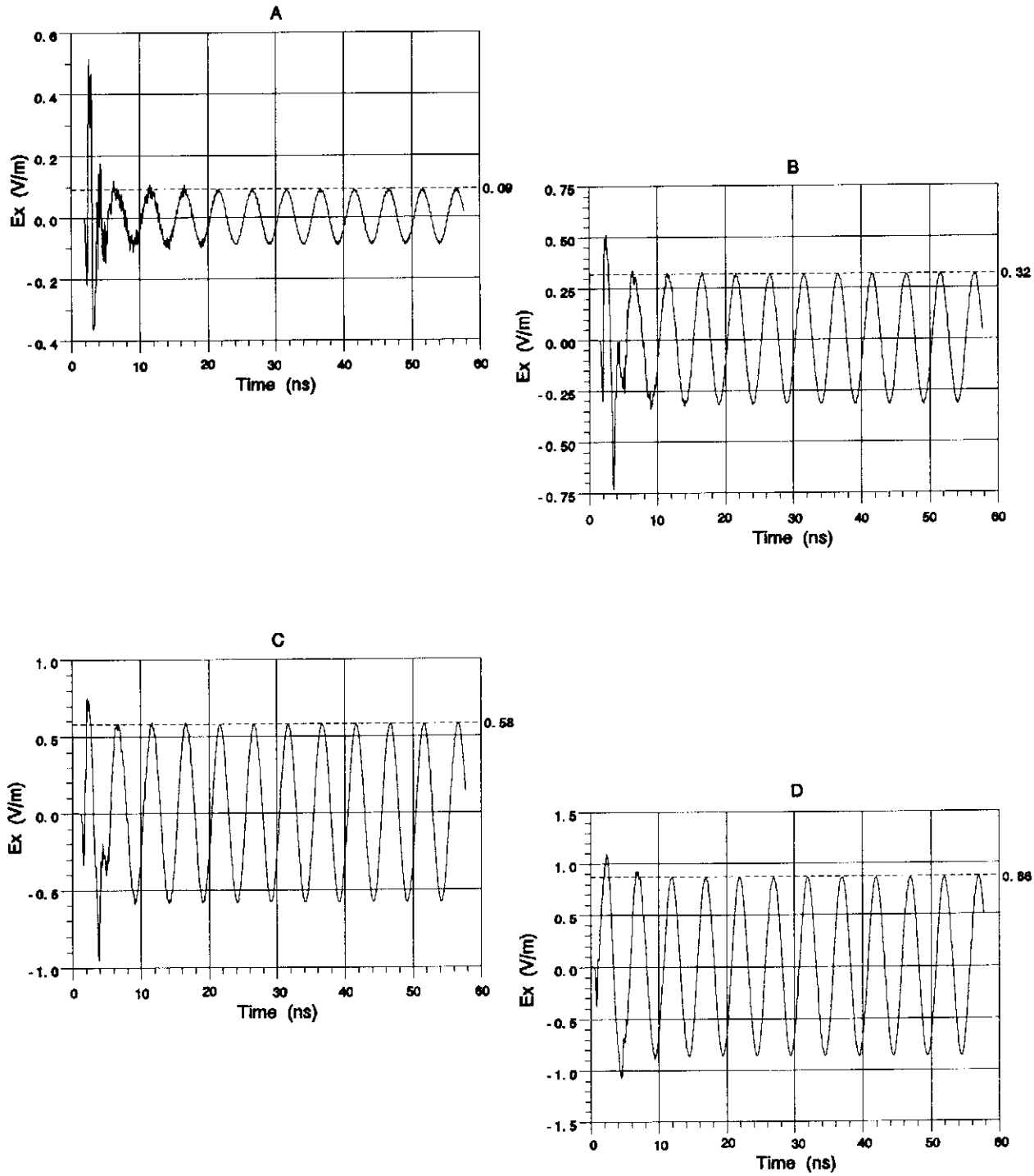

Figure 8. ...and to the sine pulse at 200 MHz.

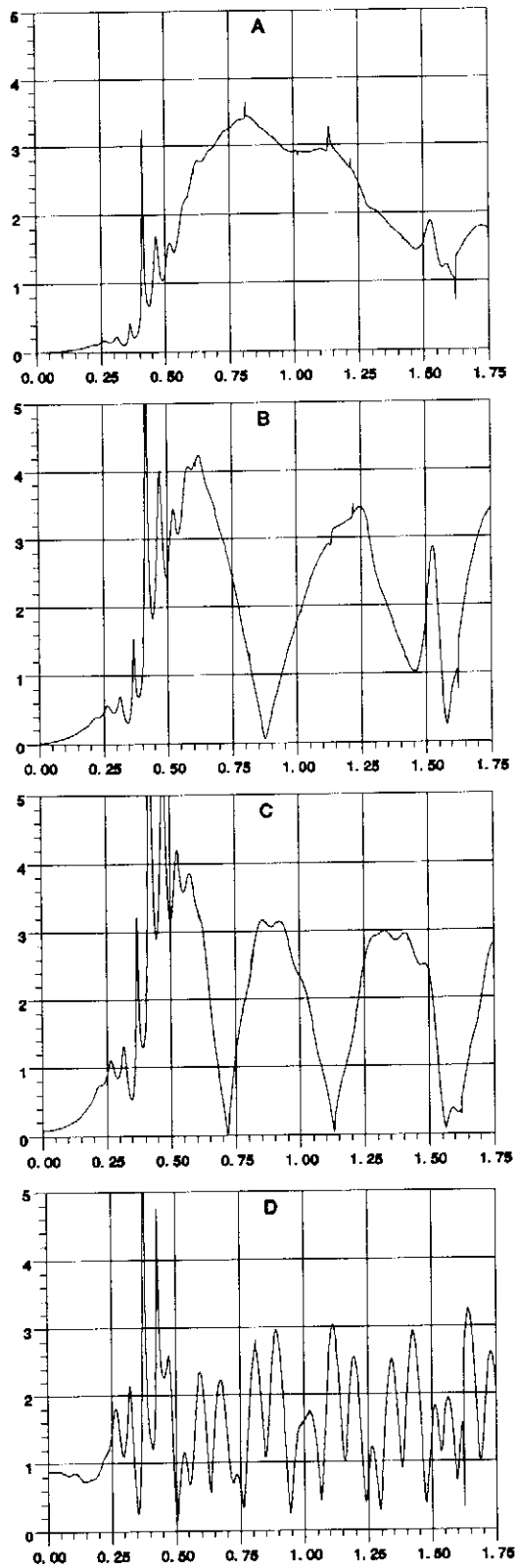

Figure 9. Fourier transforms of the curves in Figure 6 into frequency domain, with de-convolution of the incident NEMP.

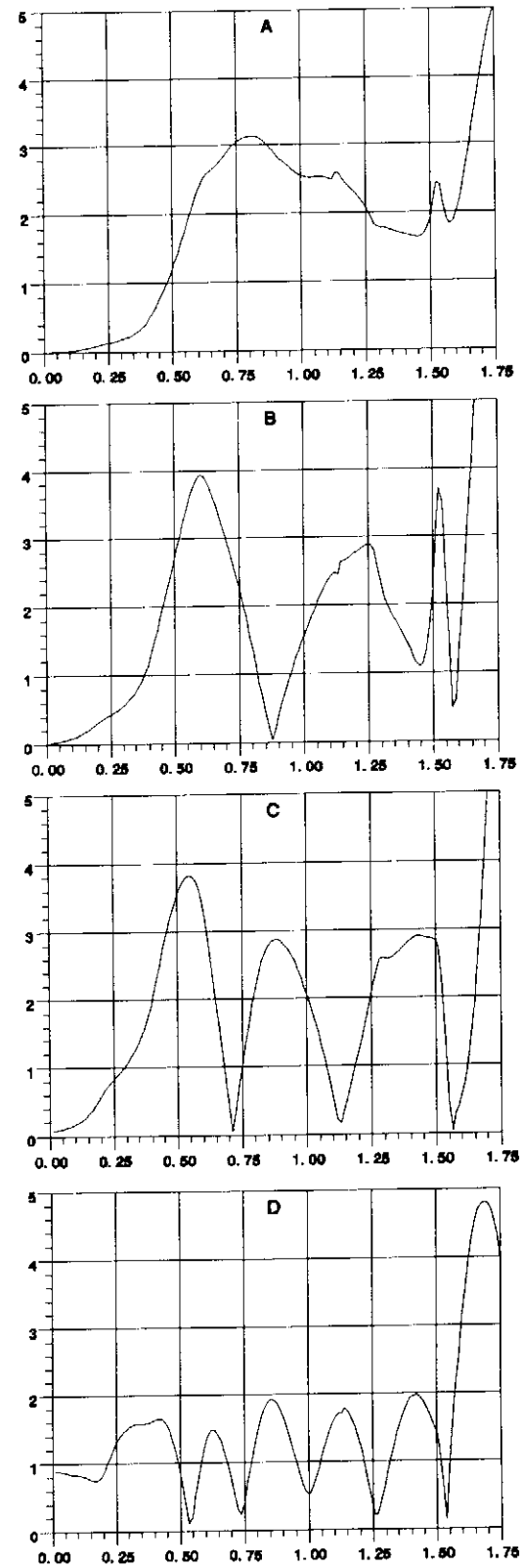

Figure 10. Fourier transforms of the curve in Figure 7 into frequency domain, with de-convolution of the incident Gaussian pulse.

[Abscissa = Frequency (GHz), Ordinate = |Ex/Einc|]

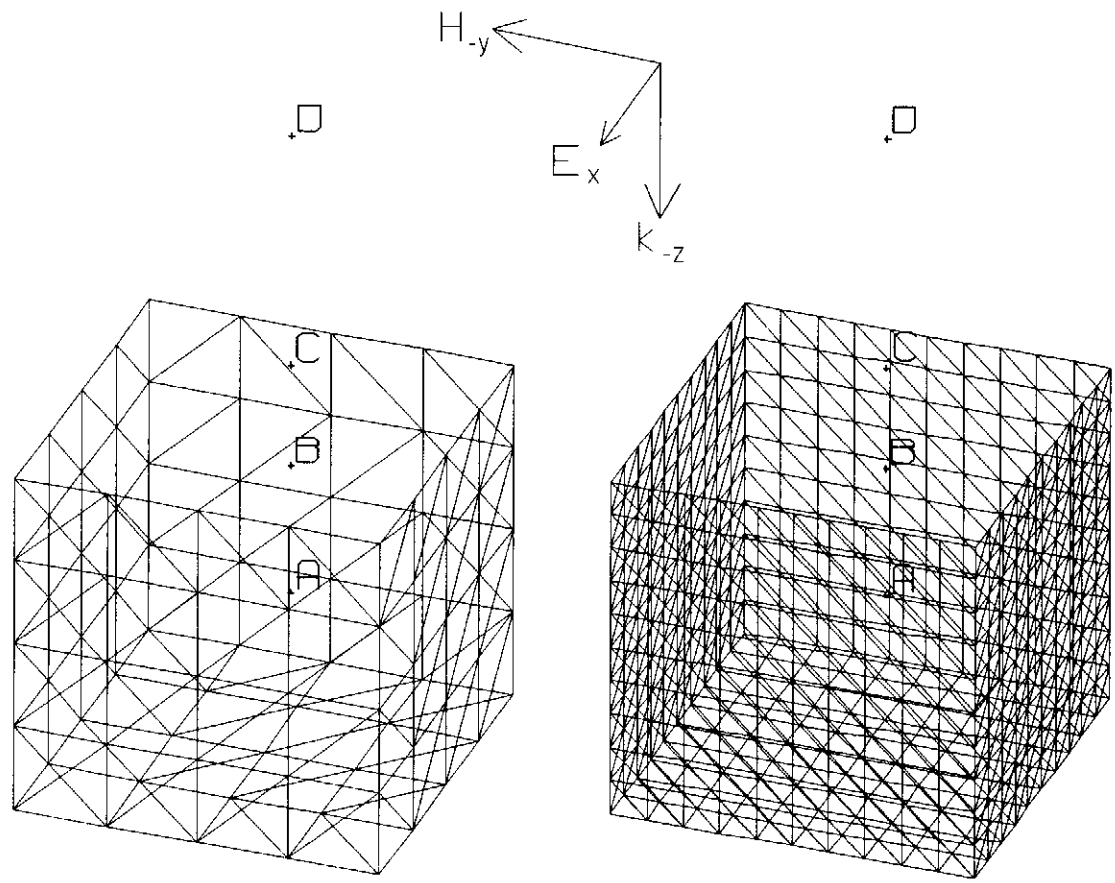

Figure 11. Two resolutions of the open-topped patch-model box used in EFIE frequency-domain studies

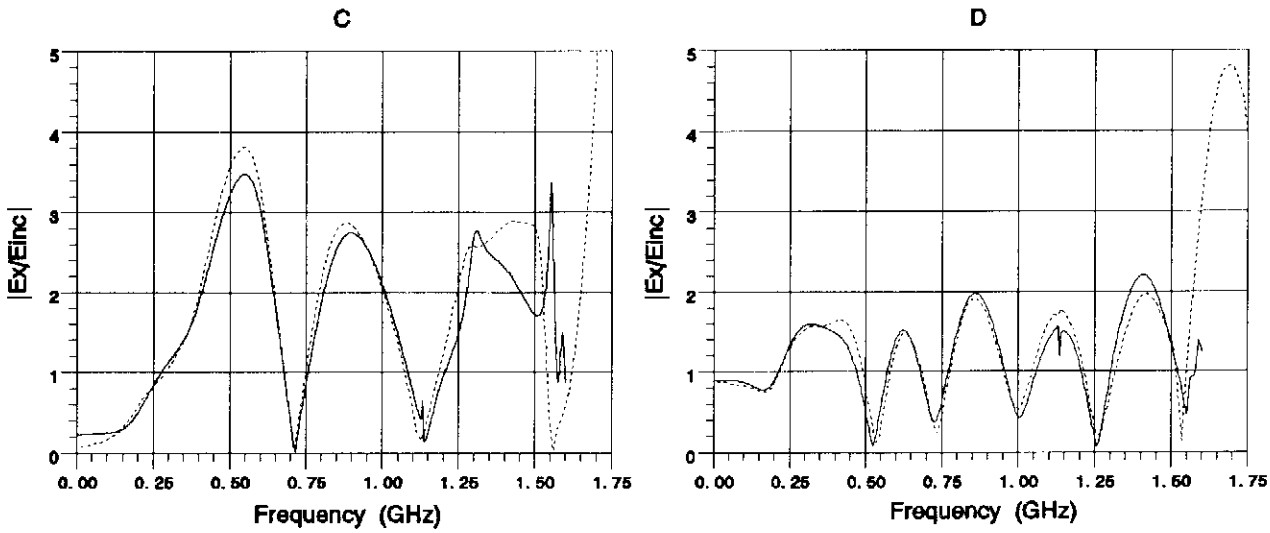

Figure 12. Comparison in frequency domain: Ex-field versus frequency at the field points C and D. Solid curve = EFIE, dashed curve = FFT(FDTD)

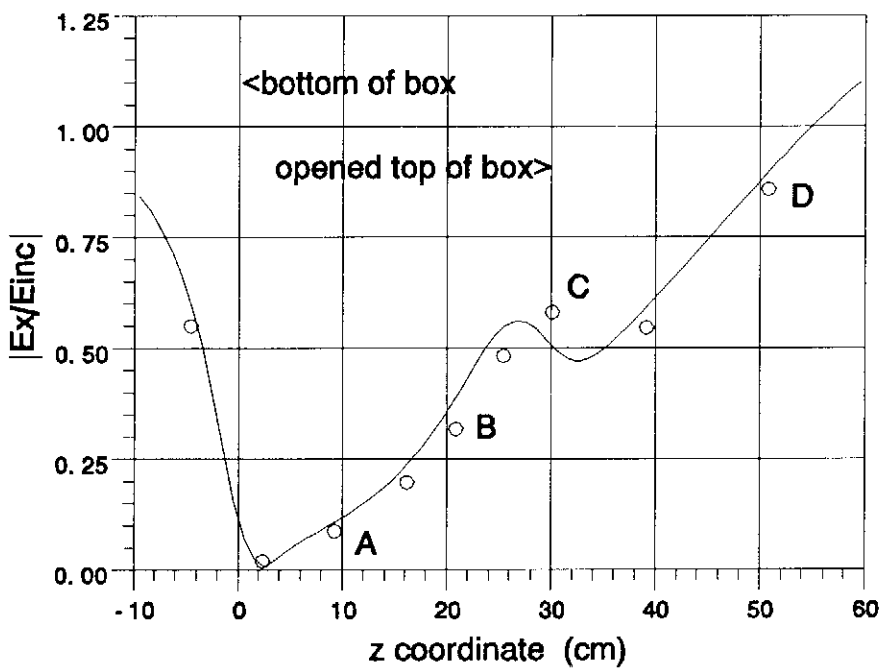

Figure 13. Comparison in frequency domain: Ex-field versus location at the frequency 200 MHz. Solid curve = EFIE, circles = FFT(FDTD)

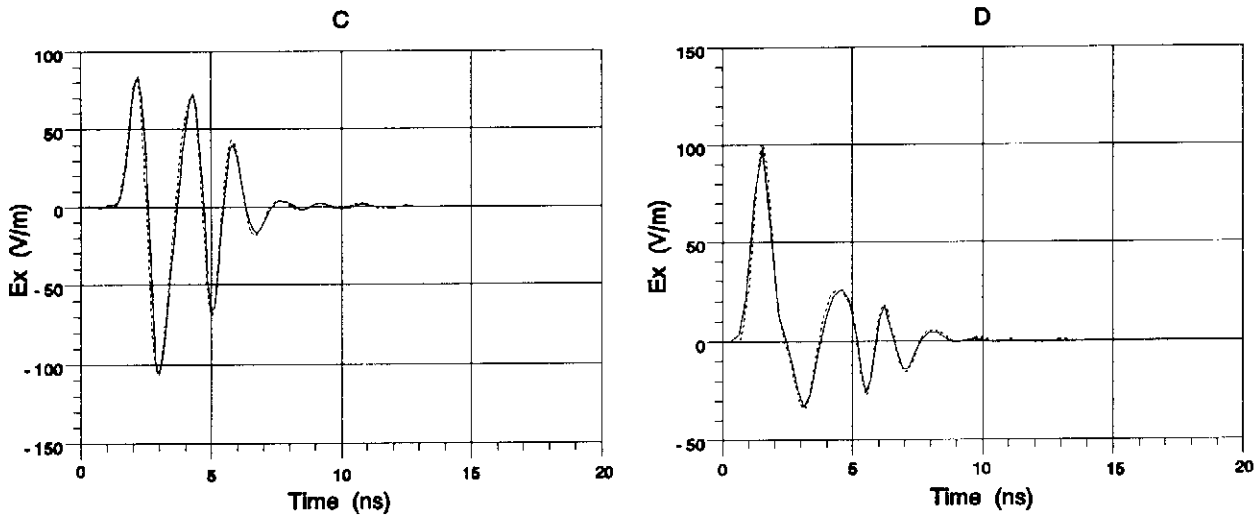

Figure 14. Comparison in time domain: Ex-field at the field points C and D. Solid curve = IFFT(EFIE)*Gaussian, dashed curve = FDTD Gaussian

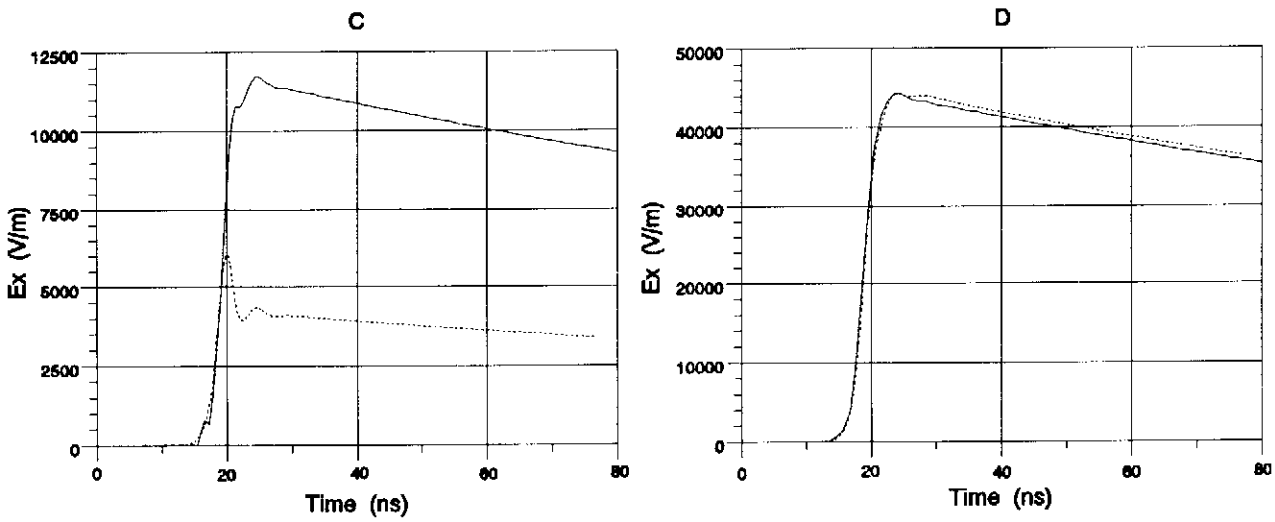

Figure 15. Comparison in time domain: Ex-field at the field points C and D. Solid curve = IFFT(EFIE)*NEMP, dashed curve = FDTD NEMP

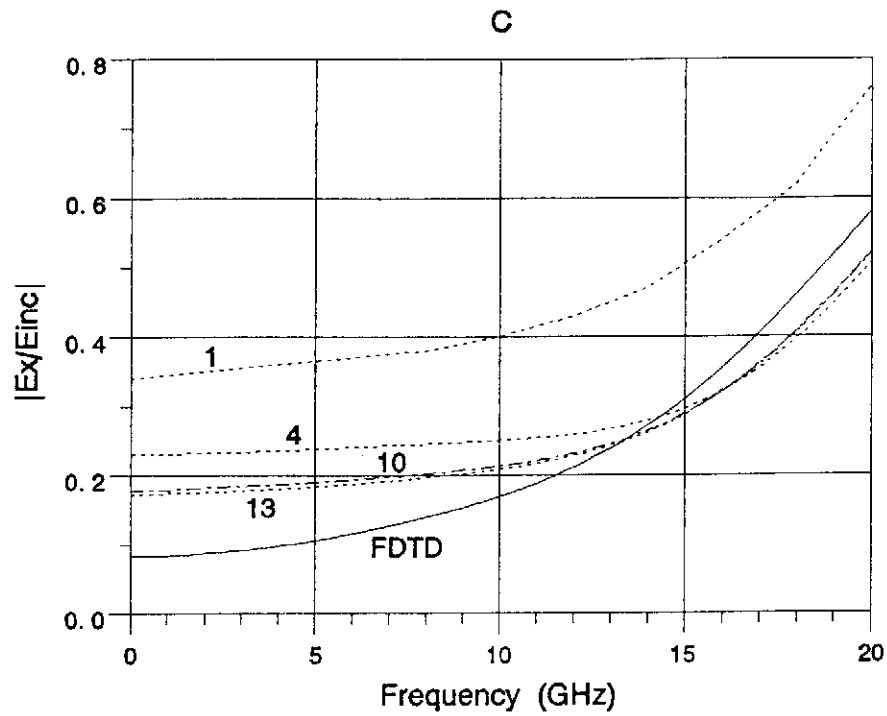

Figure 16. FFT(FDTD) compared to EFIE, in frequency domain at the field point C, with various resolutions of the patch-model box. The numbers on the dashed curves refer to the number of equal divisions of the 0.3m cubic edge.

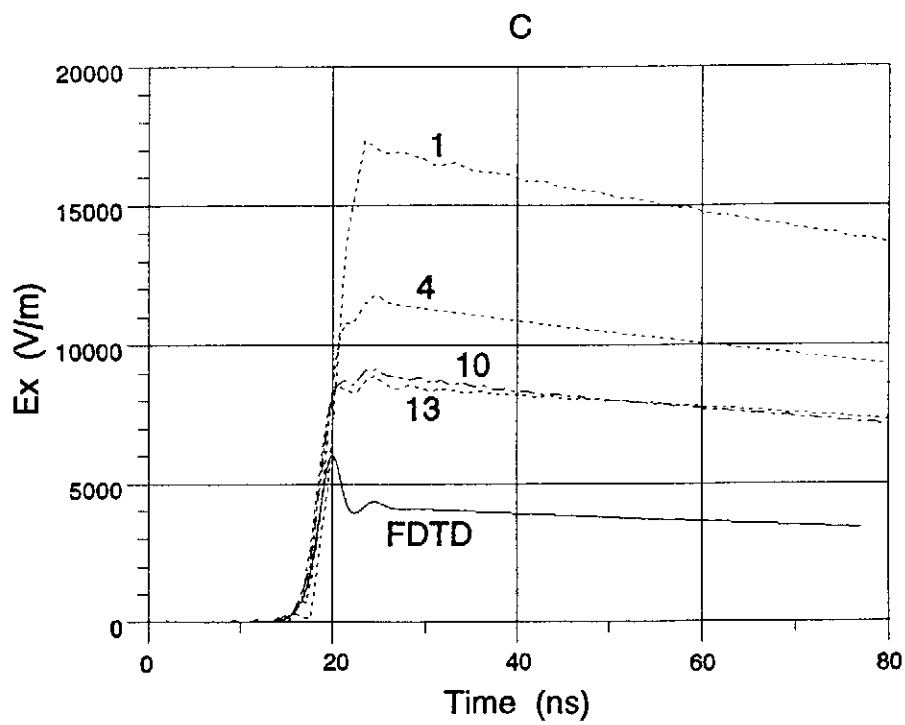

Figure 17. Inverse Fourier transforms of the curves in Figure 16: FDTD compared to IFFT(EFIE)*NEMP in time domain at the field point C. (The numbers on the dashed curves refer to the number of equal divisions of the 0.3m cubic edge.)

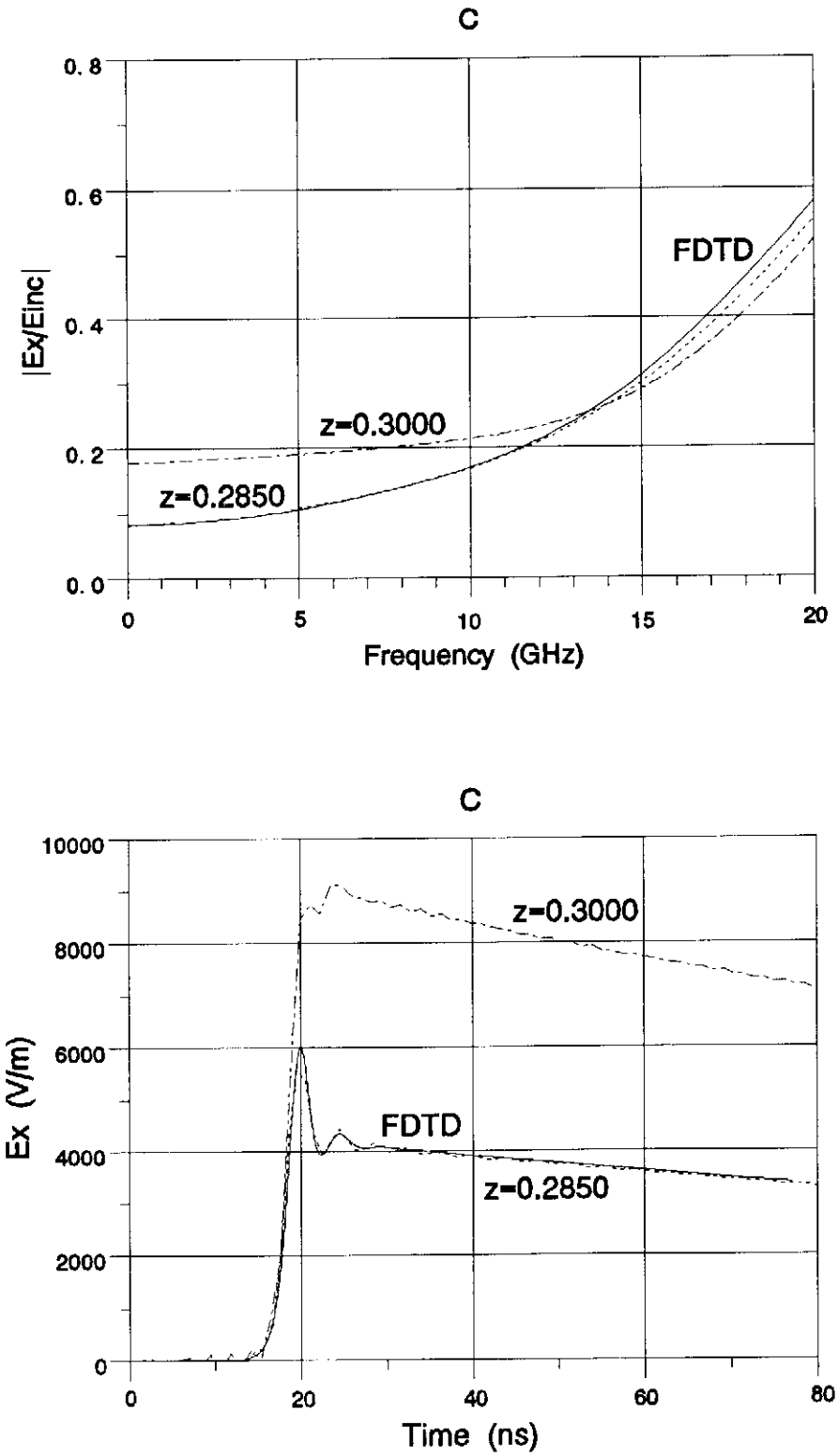

Figure 18. FDTD compared to EFIE in frequency and time domains. The best match for the FDTD field point C = (0.0577,0.1385,0.3000) is the EFIE field point C' = (0.0577,0.1385,0.2850).

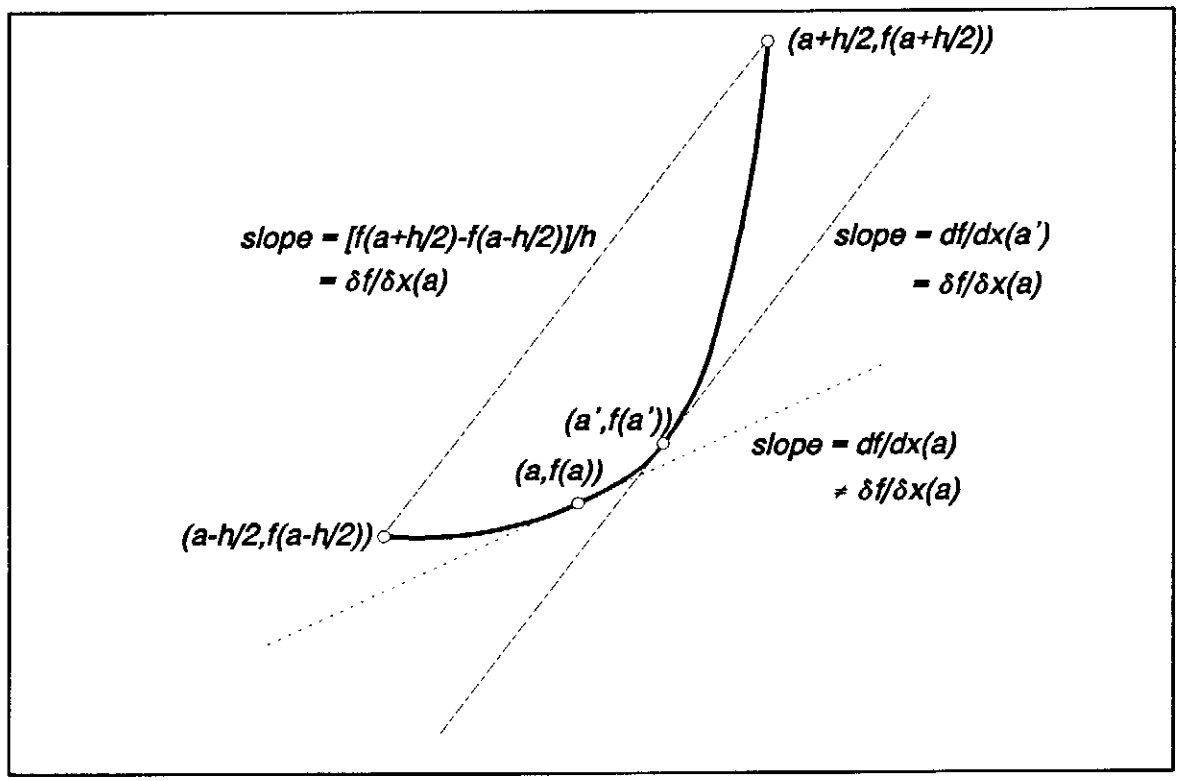

Figure 19. Illustration of the mean-value theorem for derivatives and "discretization error"